VOLVER

AN INTEGRATED QUANTITATIVE INTERPRETATION STUDY TO CHARACTERIZE SWEET SPOTS IN A SHALE-PLAY IN VACA MUERTA USING PRE-STACK AND AZIMUTHAL SEISMIC

Gabriel Chao[1], Federico Achilli[1]

1: Total Austral, gabriel.chaco@total.com, federico.achili@total.com

Keywords: **Unconventional resources, Quantitative interpretation, Elastic inversion, Brittleness index, WAZ, Azimuthal seismic**

ABSTRACT

Las características petrofísicas de los yacimientos no convencionales presentan nuevos desafíos para la caracterización de dichos reservorios en términos de que información puede extraerse de la sísmica. Los "sweet-spots" se caracterizan por una combinación de alto contenido orgánico, alta fracabilidad y alta densidad de fracturas naturales. Diferentes atributos sísmicos pueden proveer información indirecta sobre estas propiedades pero las metodologías clásicas de caracterización sísmica de reservorios deben ser adaptadas y optimizadas.

En este trabajo presentamos un estudio integrado de interpretación cuantitativa de atributos elásticos y anisotrópicos para evaluar el valor agregado de las metodologías de inversión elástica simultánea, para caracterizar contenido orgánico total y fracabilidad e, inversión acimutal para caracterizar densidad y orientación de fracturas naturales. Con este propósito, una adquisición sísmica 3D con una buena cobertura acimutal ("WAZ–wide azimuth") y un rango adecuado de "offsets" fue planificada. Uno de los objetivos principales fue la generación de cubos robustos 3D de cobertura azimutal y angular apropiada para aplicar métodos de caracterización sísmica de reservorios.

El yacimiento estudiado pertenece al bloque de la Escalonada, en la formación Quintuco-Vaca Muerta en la cuenca neuquina y su potencial ha sido probado por pozos verticales de delineación. Para la fase de desarrollo es importante optimizar la distancia entre pozos y por lo tanto la importancia de la optimización del uso cuantitativo de la sísmica 3D. Los atributos elásticos obtenidos a partir de una inversión elástica incluyen las impedancias P y S y la densidad. En este trabajo usamos un método de clasificación litosísmica para la estimación de la fracabilidad basado en los coeficientes de Lamé que nos permite independizarnos del uso del cubo invertido de densidad y obtener un atributo de fracabilidad más robusto. La intensidad y dirección de la anisotropía acimutal fueron calculadas usando la técnica de AVAz (Variación de la Amplitud con el Acimut). Estos resultados fueron comparados con la interpretación de logs de imagen disponible y atributos estructurales sísmicos que muestran la dirección principal de las fallas y lineamientos.

La interpretación integrada de los resultados demostró que la impedancia-P es un buen indicador litológico de buenas facies con valores altos de contenido orgánico y porosidad. El análisis del atributo de fracabilidad mostró resultados interesantes y consistentes con el modelo estratigráfico secuencial de la cuenca. Este atributo resultó además robusto en mapear secuencias regionales carbonáticas. Los atributos acimutales mostraron cierto grado de correlación con los logs de imagen y su interpretación converge cuando se combina con los atributos elásticos.

INTRODUCCIÓN

"La Escalonada" block, operated by Total Austral in partnership with Shell and GyP del Neuquen, is located in the center southern half of the Neuquén basin in Argentina (Figure 1). In recent years, appraisal wells have proved the potential of unconventional oil shales in "La Escalonada" at Vaca Muerta formation sequences.

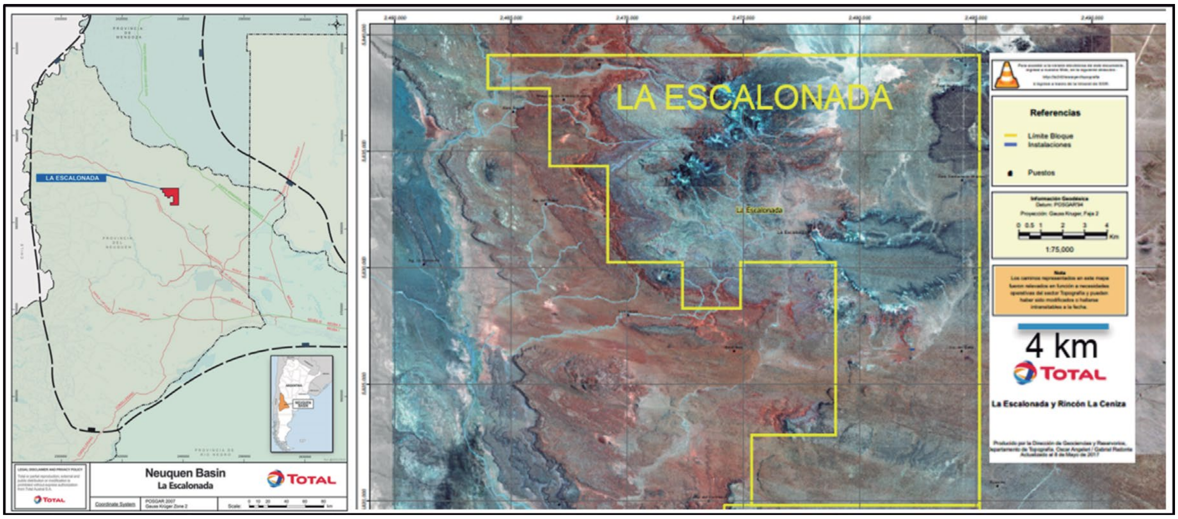

Figure 1. Location and topography of La Escalonada field.

The Vaca Muerta formation is considered as the richest source rock interval in the Neuquén basin with TOC (total organic carbon) ranging from 2 to 12 %. The shallower Quintuco formation facies are relatively poor in TOC and constitute the shallower facies of the system, which progrades from the eastern margin of the basin (Figure 2). Within this sequence stratigraphic model, three light oil-bearing "reservoir-prone" intervals are identified in La Escalonada: Sequence 7, Sequence 9 and Sequence 15-20.

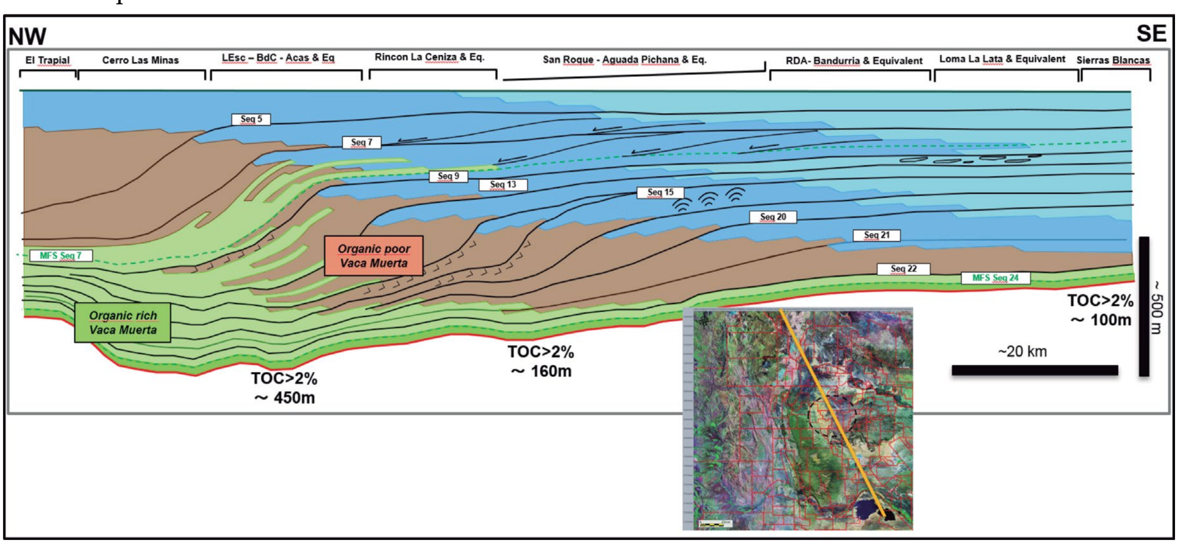

Figure 2. Regional stratigraphic sequence model of the Quintuco-Vaca Muerta formation (From Pose *et al.*, 2014).

In 2014, a 3D Wide-Azimuth (WAZ) seismic dataset was acquired in La Escalonada (Cardama *et al.*, 2015). Previously only 2D lines, mostly oriented in the E-W direction, were available in the field and only the southern part of the field was covered by 3D data. Besides the classical geophysical interpretation workflow, the purpose of this 3D WAZ acquisition was to exploit the azimuthal coverage for anisotropy and fracture characterization. Natural fracturing and microfracturing can aid hydraulic fracking in unconventional plays and therefore it can be a factor in the determination of sweet spots. The processing sequence of the data focused on preserving the azimuthal information.

Figure 3 shows the improvement of the 3D WAZ seismic with respect to the previous 2D lines. Higher signal to noise ratio and an increase in frequency content are evident.

The objective of this study is to analyze with a critical view the value of information of azimuthal and pre-stack seismic data for the characterization of TOC, brittleness and fracture distribution in La Escalonada block in order to benefit from the potential of these techniques and understand their limitations in the determination of the drains location, azimuth, spacing between wells, drain length and landing intervals.

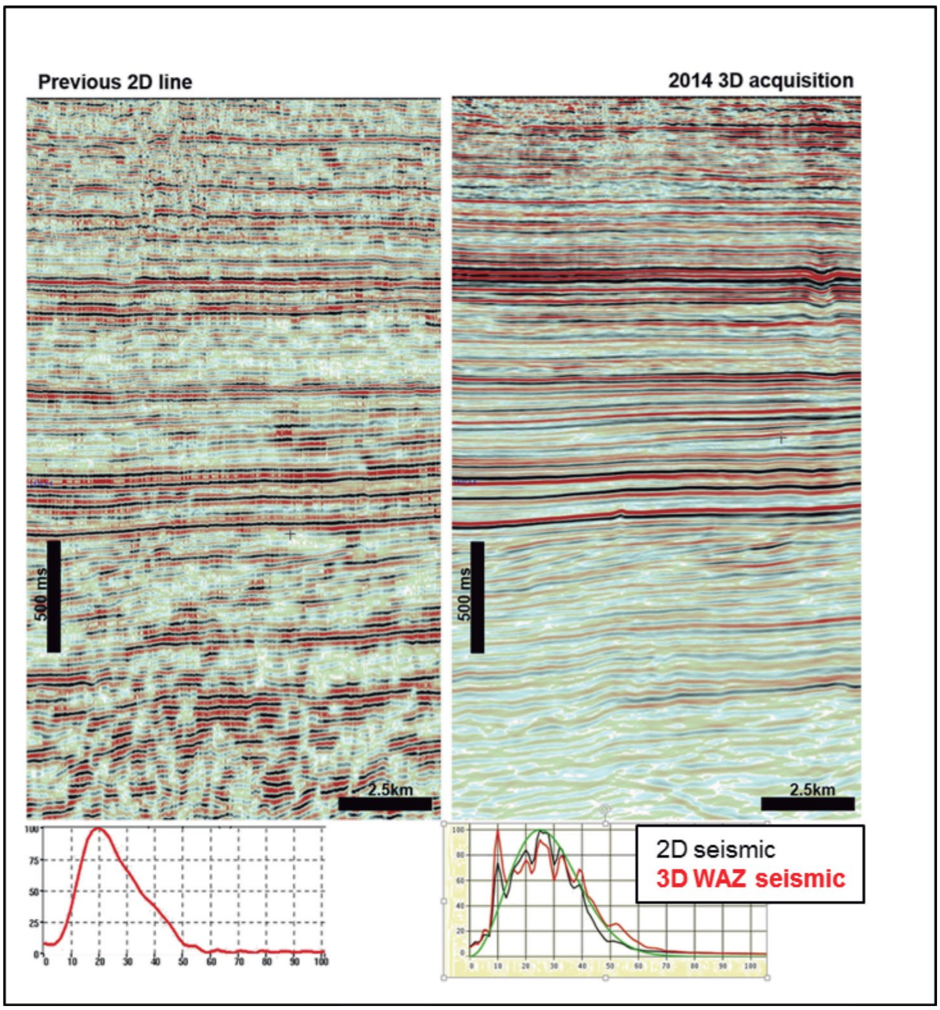

Figure 3. Comparison of previous 2D line and the 3D WAZ acquired in 2014 (from Borgnia, 2016).

Quantitative Interpretation techniques

The final dataset for quantitative reservoir characterization included six azimuth sectors with three offset angle stack per azimuth. The angle ranges for the azimuths (in clockwise direction from the North) were: 0°-30°, 30°-60°, 60°-90°, 90°-120°, 120°-150° and 150°-180°. The coverage of the angle stack were: Near, 5°-15°; Mid, 15°-25°; and Far, 25°-35°. Three wells with a full set of elastic and petrophysical logs were available for preconditioning of the data, wavelet extraction, low-frequency model building and QC.

AVAz analysis for fracture characterization.

The AVAz attributes computed are based on the Ruger´s equation (Ruger, 1997) for the variation of reflectivity with azimuth and incidence (offset) angle:

$$R(\varphi,\theta) = A + \left[B^{iso} + B^{ani}cos^2(\varphi - \varphi_0)\right] sin^2\theta \qquad (1),$$

where R is the P-wave reflectivity, φ is the azimuth angle, θ is the incidence angle, A is the AVO intercept, Biso is the AVO gradient, Bani is the anisotropic gradient and φ_0 is the anisotropic orientation.

Ruger´s equation is an extension of the Shuey´s equation (Shuey, 1986) to account for HTI anisotropy. In geological terms, this type of anisotropy is characterized by a set of parallel planes perpendicular to the bedding and it is commonly used to modeled the effect of (quasi-)vertical fracture networks. The effect of anisotropy is more significant at large offsets. Therefore, the six azimuth cubes of the Far substack angle were used to perform the AVAz study. In practice, the azimuthal variations of the seismic amplitudes are fitted to equation (1) using a least-squares algorithm. An example of the azimuthal dependence of the amplitudes is shown in Figure 4 where the anisotropic effect can be clearly seen at key intervals. The azimuthal data was aligned through the computation of 3D time shift cubes. This is equivalent to residual move-out and it is a key step to align the events and to obtain meaningful AVAz results. The output of the AVAz inversion are the anisotropic gradient B^{ani} and the anisotropic orientation φ_0. The anisotropic gradient is an indicator of the strength of the anisotropy that can be related with the fracture density. The attribute φ_0 is related to the direction of anisotropy and can be linked with the orientation of the fracture network. The analysis of these attributes has to be supported with image data at well locations that confirm the assumption of natural fractures as the main cause for anisotropy. It is important to keep in mind that regional (or local) stresses and acquisition footprint may also induce anisotropy in the seismic signal. One of the main uncertainties of this method is that both φ_0 and φ_0+ 90° are possible solutions to equation 1 given the same set of azimuth input amplitudes. It is therefore very important to introduce some a-priori geological knowledge of the fracture network in order to constraint the solution to a meaningful strike orientation. In Section "Results and Interpretation" it is discussed how this was handled in La Escalonada.

Elastic Inversion and seismic classification for brittleness and TOC characterisation

A model-based elastic inversion was performed using the three angle stacks available: Near (5°-15°), Mid (15°-25°) and Far (25°-35°). The three wells available were used to extract the wavelets and build the low-frequency model. Residual normal move-out was applied to align the substacks prior to simultaneous inversion. The initial low-frequency model was built using log data kriged following the structural framework determined by the interpreted horizons. The wavelets were extracted using a least-square algorithm to invert for a frequency-dependent phase wavelet that match a reference trace built after stacking the neighboring traces around the wells.

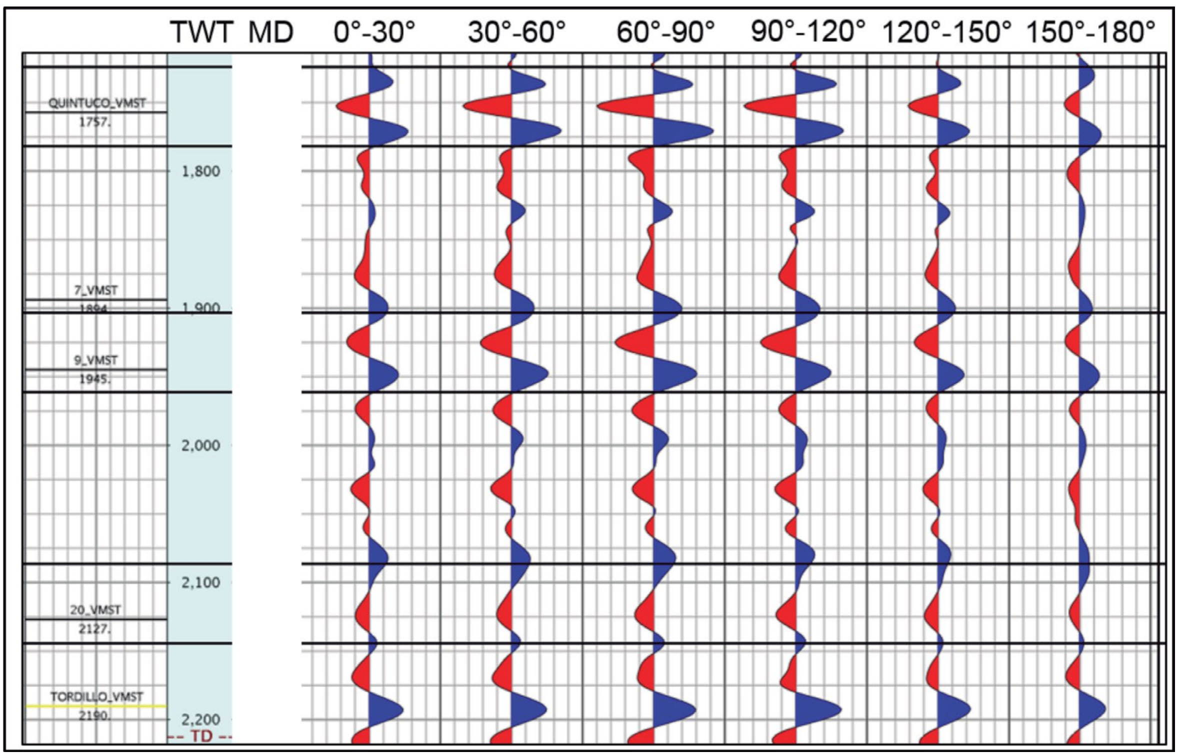

Figure 4. An example of the observed amplitude variation with azimuth in one of the wells. These amplitudes are the input to the least-square inversion for Ruger´s equation (Equation 1) from where the 3D anisotropic attributes, anisotropic gradient and anisotropic orientation are obtained. Intervals of interest are highlighted.

The output of the elastic inversion are the elastic properties of the reservoir: acoustic impedance (AI), shear wave impedance (SI) and density. For interpretation purposes sometimes Poisson ratio (PR) and VpVs ratio are preferred and can be directly obtained from AI and SI. Poisson ratio can be used as an indirect indicator of fracability (more brittle rocks tend to have a low Poisson ratio).

The density cube is in most cases noisy and not robust since the range of angles needed to obtain a robust and reliable density cube is too high and not attainable in most acquisitions, neither in this case.

The elastic inversion results and intermediate computations were QCed using industry standards: quantitative analysis of the seismic-well calibration during the wavelet extraction per substack, analysis of the prediction at well locations against elastic computed logs and filtered to the seismic bandwidth, analysis of residuals magnitude and frequency content for each of the input cubes. The match between the elastic attributes and the log data was good with correlation coefficients above 0.7. The residuals were low and did not present significant geological character. From an interpretation point of view, key sections and maps were analyzed. Figure 5 shows a North-West to South-East cross section with the AI and SI results. The progradations in the stratigraphic sequence model are nicely reproduced by both the acoustic and shear wave impedance attributes, especially the resolution of the SI is very good and allows characterizing the progradations quite accurately. Both quantitative and interpretative QC were positive and gave confidence on the quality of the computed attributes for their use in quantitative interpretation and further in seismic classification for brittleness index.

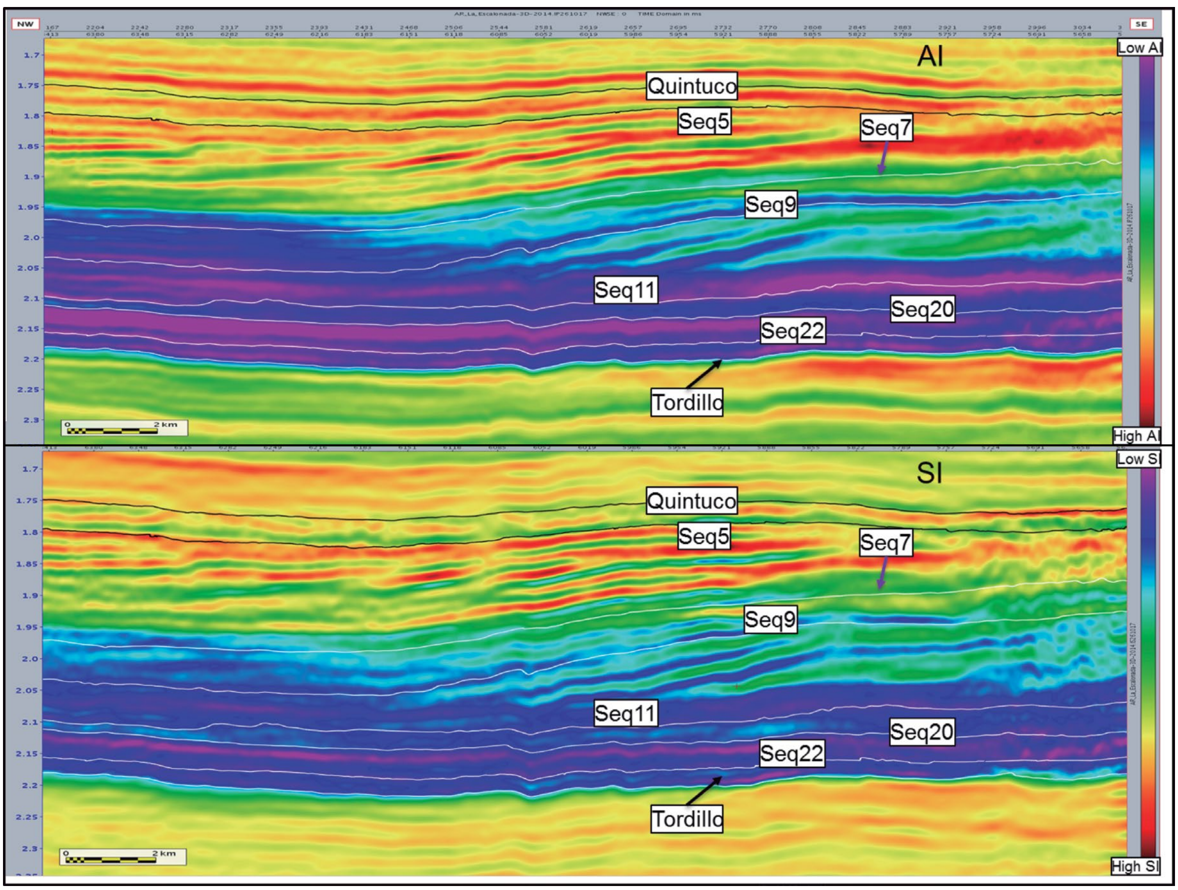

Figure 5. Acoustic Impedance (AI, top) and Shear Impedance (SI, below) from elastic inversion along a NW-SE line. The progradations are nicely reproduced by both attributes and are consistent with the stratigraphic sequence model (Figure 2).

Brittleness Index estimation

Since rocks with higher brittleness are easier to fracture than rocks with lower brittleness, there is a geological and engineering interest in mapping an estimation of this geomechanical property. Moreover, more ductile shales (low brittleness) tend to heal induced fractures and may act as barriers for fluid flow. In unconventional plays there have been several studies in the last years where estimation of brittleness/fracability is obtained from the elastic attributes products of an elastic inversion (see e.g. Vargas *et al.*, 2012). However, most of these studies make use of the density cube to compute the Young modulus, which is later used as an input in a classification scheme to obtain the brittleness index in the PR vs Young Modulus domain. As mentioned earlier, the poor confidence of the density cube after elastic inversion implies a high uncertainty in the results for the brittleness index.

In this study we prefer to use a seismic classification for brittleness index (BI) based on a classification in the $\lambda\rho$, $\mu\rho$ domain (λ and μ are the Lamé coefficients) (Perez *et al.*, 2014). The elastic parameters $\lambda\rho$, $\mu\rho$ can be obtained from seismic AI and SI without the use of the density attribute with the following equations:

$$\lambda\rho = AI^2 - 2SI^2, \text{ and, } \mu\rho = SI^2. \qquad (2)$$

The potential of these attributes to discriminate BI was analyzed using log data. The idea was to analyze if the mineralogic brittleness index computed at the wells with cuttings was properly discriminated in the $\mu\rho$ vs $\lambda\rho$ crossplot based on log data. If this is the case then we could build an operator and use it in a seismic classification scheme to estimate BI from the output of the seismic inversion. In the three wells, full sonic data was available to compute the $\lambda\rho$ and $\mu\rho$ elastic attributes. To compute the brittleness index we used the method proposed by Wang *et al.* (2009) that is based on the mineralogic composition of the shales. In this formulation the brittleness index is defined as the fraction of brittle mineral in the rock. A full mineralogic analysis was available in the three wells and the brittleness index was defined as:

$$BI = {(Vol_{calcite} + Vol_{quartz} + Vol_{pyrite})}/{(Vol_{illite} + Vol_{calcite} + Vol_{quartz} + Vol_{pyrite} + Vol_{kerogen} + PHI_{total})}, \qquad (3)$$

where $Vol_{calcite}$, Vol_{quartz} and Vol_{pyrite} correspond to the fraction volumes of the brittle minerals calcite, quartz and pyrite respectively. The denominator serves to normalize the definition of brittleness. The results are shown in Figure 6 (left).

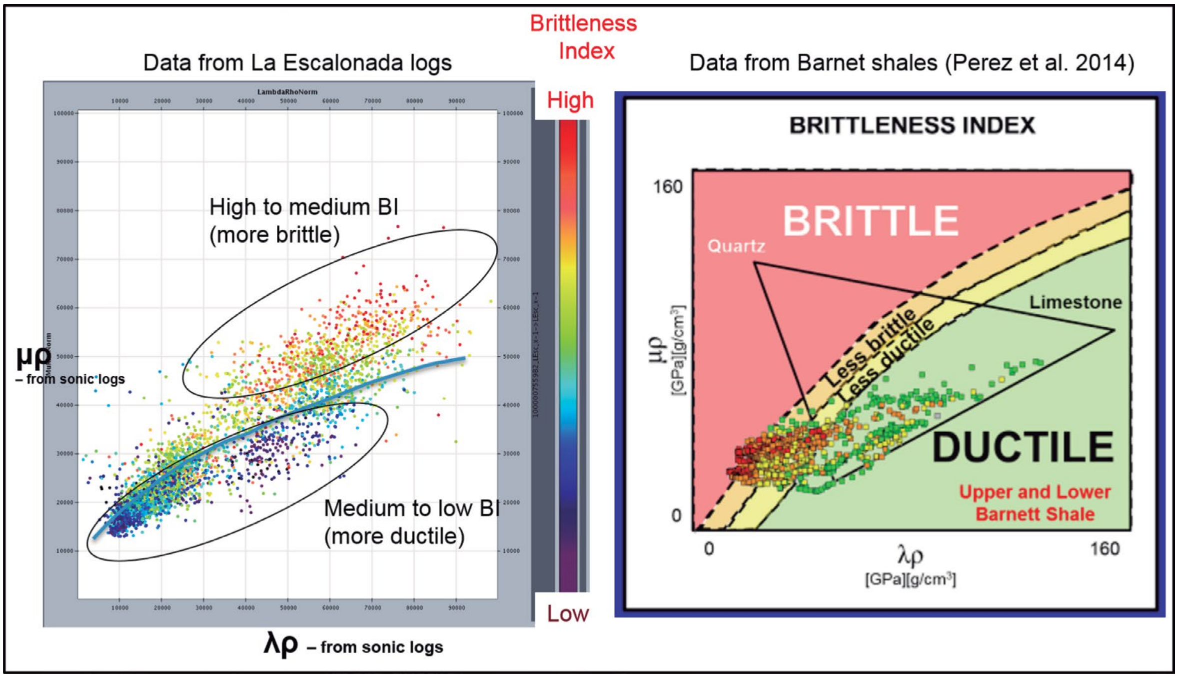

Figure 6. Sensitivity of the brittleness index in the μρ vs λρ well (logs and cuttings) domain. Data from Barnet shales (from Perez *et al*, 2014) shows the same qualitative behavior than shales from La Escalonada. Two brittle regimes are distinguished and can be properly discriminated.

The sensitivity study to discriminate mineralogic brittleness index using cutting data allowed discriminating the different regimes in the μρ vs λρ log domain (Figure 6). Two regimes can be qualitatively discriminated. These results were compared to published data available in the literature from the Barnet shales (Perez *et al.*, 2014), where the same behavior was observed.

Using the Kernel Density Estimation method (Scott, 1992), an operator from log to seismic μρ, λρ was built that was later used to map the computed λρ, μρ attributes obtained from the elastic inversion results (through equations 2) into the mineralogic brittleness index. The resulting operator is shown in Figure 7. In this way a 3D BI cube was obtained that was used later on in the integrated interpretation of the results together with the anisotropic attributes.

Results and Interpretation

The interpretation approach was based in the joint analysis of the attributes computed: acoustic impedance (AI), shear-wave impedance (SI), Poisson ratio (PR), brittleness index (BI), anisotropic gradient (Bani) and anisotropy direction (φ0). These attributes were interpreted and analyzed considering all available log data, including interpreted electrofacies and image logs that are crucial to QC the seismic results in terms of fracture prediction.

Figure 8 shows the AI results from the pre-stack inversion along a West-East line intersecting two of the appraisal wells. The progradation geometry of the facies mapped by the inverted AI is

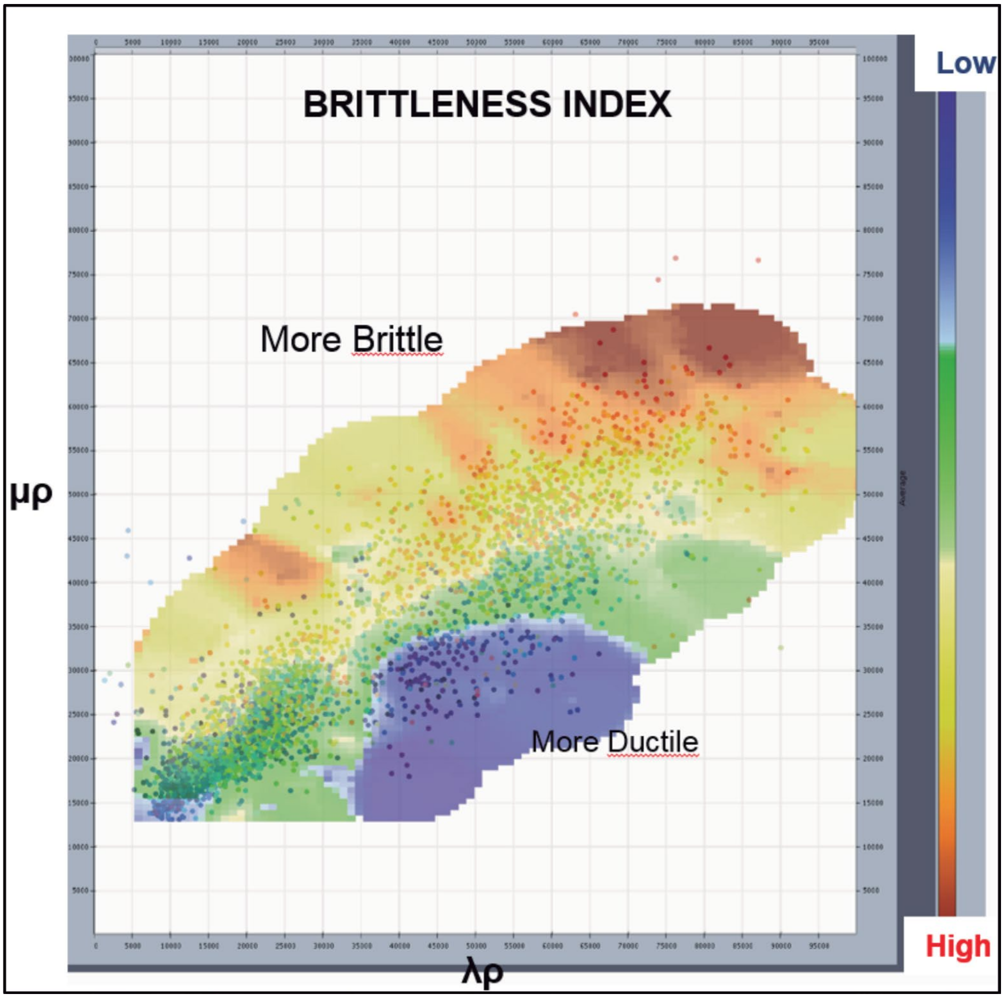

Figure 7. BI operator computed using log data from the crossplot of Figure 6 (left). The Kernel Density Estimation method was used to compute the well to seismic operator. The resulting operator is overlaid with the well input data points.

consistent with the regional stratigraphic sequence model of the basin with platform carbonate facies that prograde or agrade from East to West (hot colors, high AI). The AI attribute is used as an indicator of TOC and porosity: low values of AI are associated with high values of TOC and porosity. In one of the appraisal wells, Well-C, a complete electrofacies interpretation is available. Using sonic and density log data, the sensitivity of the electrofacies in the VpVs ratio vs AI was studied. From the crossplot it can be concluded that the AI attribute is a very good indicator of carbonate facies, there is a clear cut-off for AI, above which only carbonate facies are mapped. On the other hand the best facies, the siliceous claystone/mudstone/wackestone are mostly mapped in the low AI range.

The inverted AI results showed a good correspondence with the interpreted electrofacies and the petroelastic analysis based on the VpVs ratio vs AI crossplot (top right). At the base of the stratigraphic unit between Sequence 5 and Sequence 7, a set of high AI layers are obtained which correspond to the carbonate facies interpreted at the Well-C location (1). The inverted AI predicts

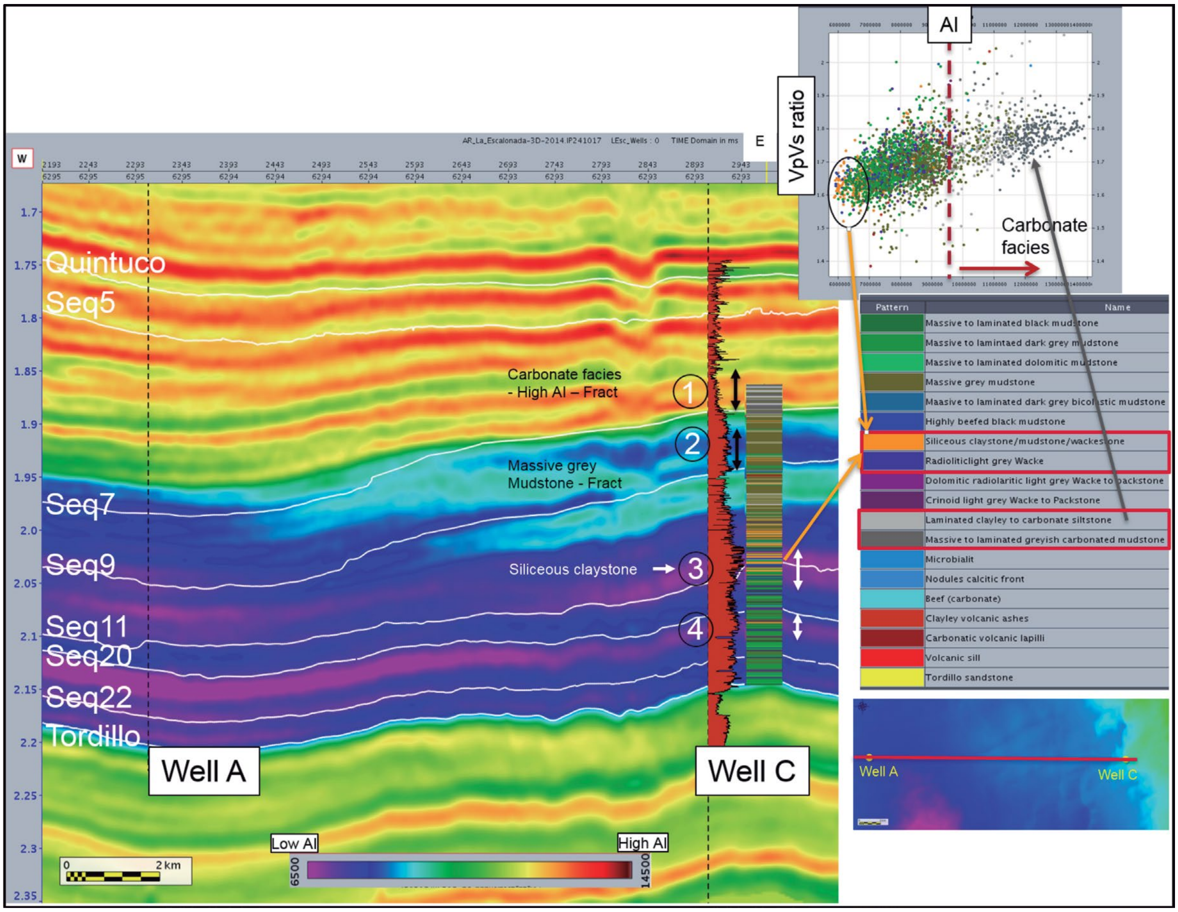

Figure 8. A West-East section of Acoustic Impedance after Elastic Inversion. The electrofacies interpretation for Well-C is shown together with the TOC log. The elastic response of the electrofacies in the VpVs ratio vs AI domain is also shown (top right). The map of the isochron at Top Tordillo is shown for reference.

three intervals of low AI (high TOC): in Sequence 7 (2), above the top of Sequence 11 (3) and in Sequence 20 (4).

From these observations we can conclude that the AI is, overall, a good lithological indicator in La Escalonada. However, sweet-spots are not only characterized by good facies but also by how easy these facies can be fracked and the existence of natural fractures can enhance the stimulated fracture network generated during hydraulic fracturing. The seismic generated brittleness index and anisotropic attributes were analyzed to complete the characterization of sweet spots.

Figure 9 shows the brittleness index results obtained using the seismic classification operator displayed in Figure 7 using as input the λρ, μρ attributes derived from the AI and SI outputs of the elastic inversion. The line intersects wells Well-A and Well-C. In both wells, formation image logging (FMI) was performed which allowed characterizing the main features of the natural fractures. The fracture density is displayed along the wells with the same normalization, this means that Well-C encountered far more fractures than Well-A.

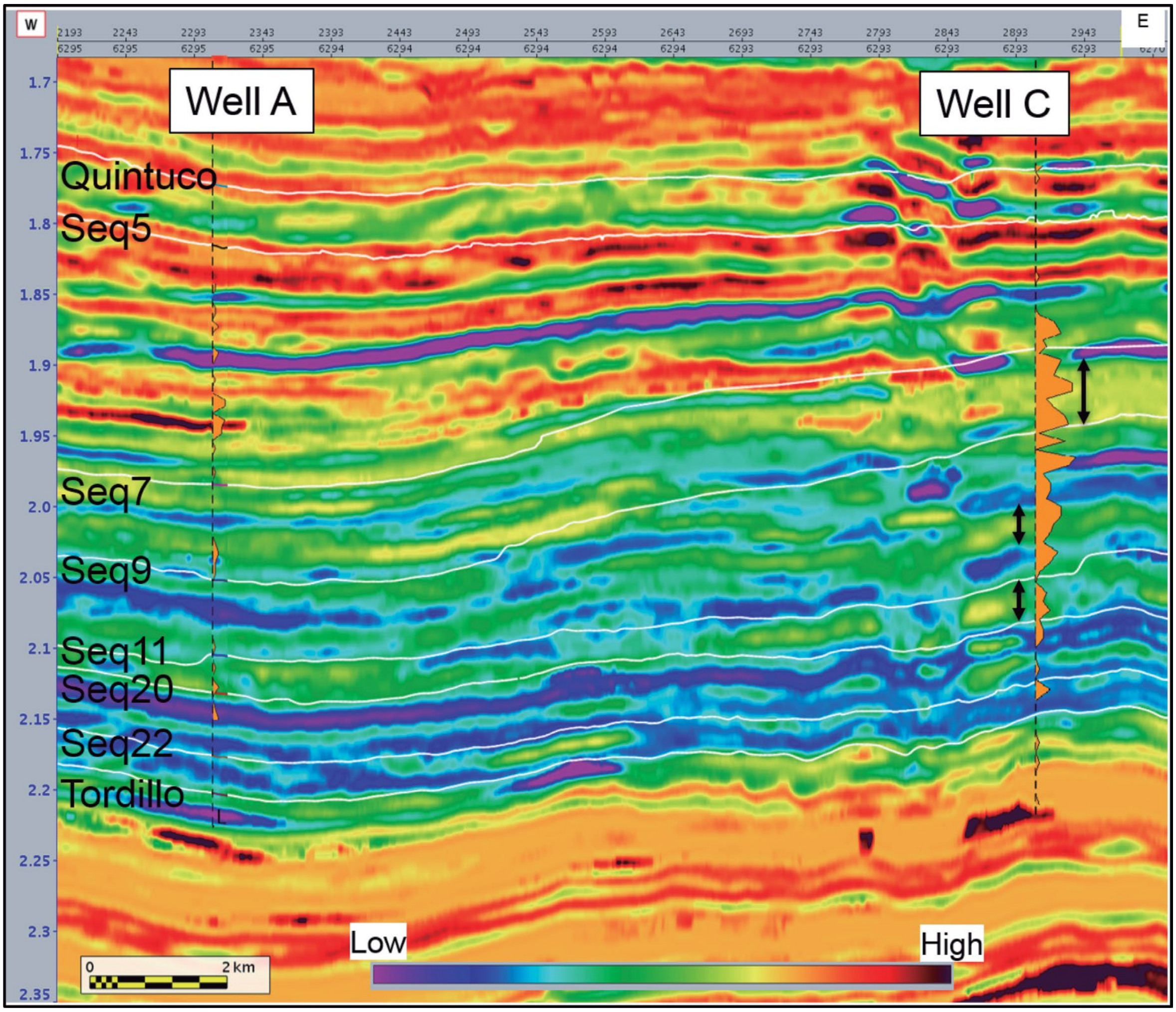

Figure 9. Brittleness index along an East-West line intersecting Well-C and Well-A. The interpreted fracture density from the FMI data are shown in orange along the well trajectory.

We observed that the seismic BI respects quite nicely the geometry of the progradations with carbonatic platform facies of Quintuco (in hot colors) with high BI and slope and basinal facies of Vaca Muerta formation with low BI (cold colors). The BI seismic attribute shows high values in Sequence 7 and Sequence 9 at well location Well-C. These intervals are characterized by massive grey sandstone facies which are brittle. The seismic BI also predicts intervals of relative high brittleness within the sequences 11 to 20. In general we noted an overall qualitative correspondence between the seismic BI index and the fracture density from the FMI. The seismic BI seems to qualitatively map intervals of brittle rocks characterized by a high fracture density. This serves as a good QC because although the fracture density and the brittleness are related physically, the fracture density information is not used at all for the calibration of the BI index operator.

Another qualitative QC for the seismic BI is the analysis of the results at the Tordillo level. The Tordillo is known to be a tight and more brittle formation with seismic faults clearly visible in amplitudes sections and in structural attributes such as coherency and curvature. The seismic BI is consistent with these observations as it predicts a high brittleness below the Top Tordillo. It also predicts the Tordillo being more brittle towards the East than the West. This seems consistent with observations from cuttings where a more continental character of the facies were observed at the Tordillo level in the Well-C. The cuttings of Well-A also showed abundant argillaceous matrix in the sandstones at Tordillo level that may correspond to a more ductile rock compared to the cleaner sandstones in Well-C.

The use of the seismic BI in combination with the AI seems a good strategy to characterize the sweet spots in La Escalonada (good lithological facies with the tendency to be fracked).

Figure 10 shows the same section for the anisotropic gradient, Bani, obtained through the AVAz inversion of equation 1. The low frequency character of the attribute is related to the choice of azimuths of the Far substack as input in order to maximize the impact of anisotropy and obtained more robust results. The attribute shows a trend of increasing anisotropy towards the

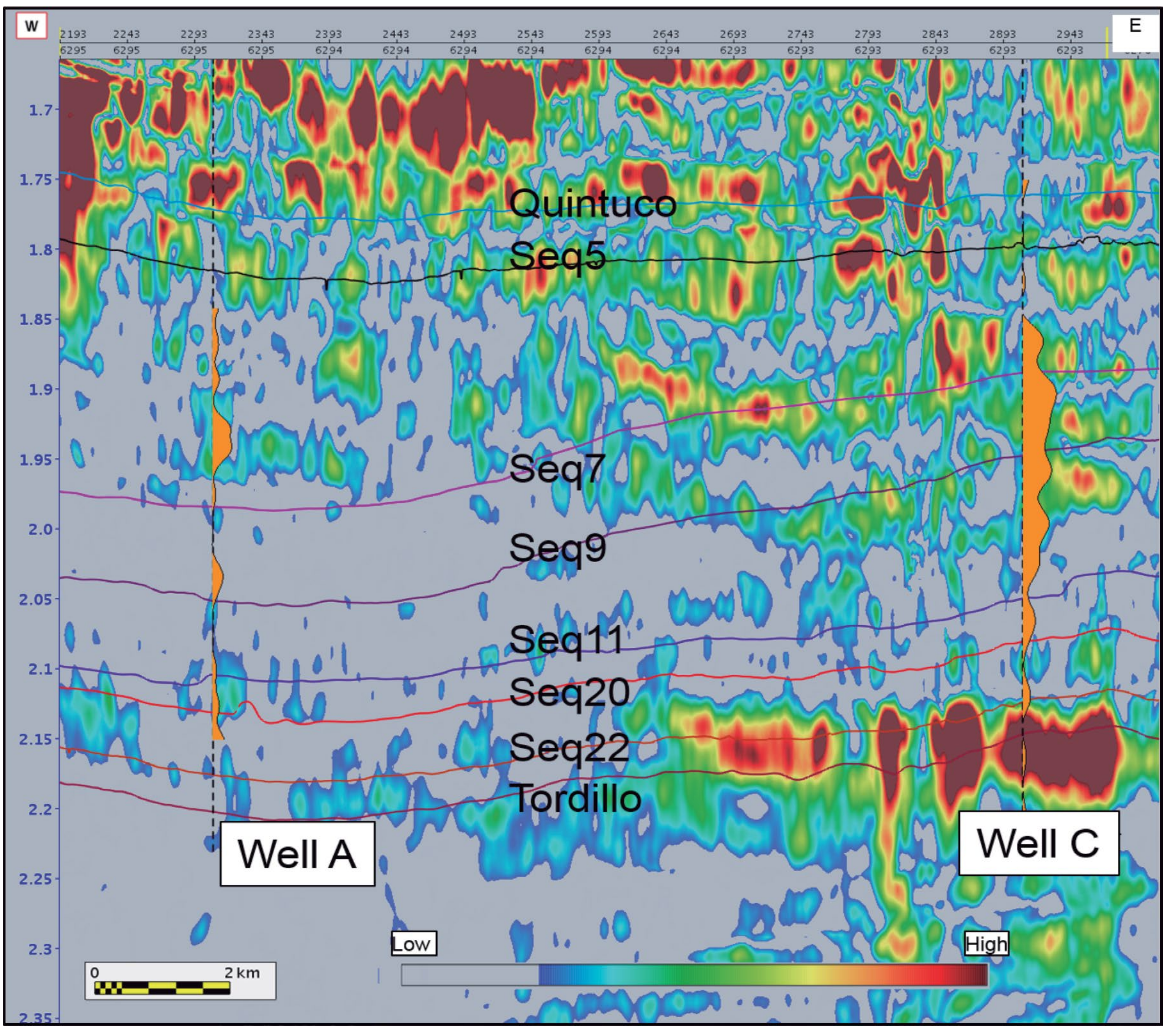

Figure 10. Anisotropic gradient, Bani along an East-West line intersecting Well-A and Well-C. The interpreted fracture density from the FMI data filtered within the Far substack seismic bandwidth (high-cut: 30 Hz) is shown.

East, which is consistent with the existing evidence of increasing fracturing from the comparison of the FMI logs in Well-A and Well-C. This trend is also consistent with the seismic BI results discussed previously. The lateral variation of the anisotropic gradient is also consistent with the seismic BI results.

The analysis of the FMI results at Well-C and the comparison with the anisotropic attributes derived from seismic is shown in Figure 11. The fracture density from the FMI logs was filtered in the seismic bandwidth to be able to compare it with the seismic attributes. The main findings from the FMI log showed a predominant set of fractures with an East-West azimuth and a fracture dip close to 80°. This allowed us to validate to certain extent the hypothesis behind Ruger's equation which is valid, in principle, for a single set of vertical fractures. The anisotropic gradient Bani and the fracture orientation computed from the seismic data are extracted along the well for comparison. Three main intervals can be identified. The shallowest one (from above Sequence 5 to above Sequence 9) is characterized by a clear N°90°E azimuth that is quite clearly reproduced by the seismic orientation attribute. The second interval is a thin one (around 10 m thickness) with a N°60°E orientation observed in the FMI. In this interval, there is no agreement with the strike from seismic. In the third interval (from above Sequence 9 to Tordillo) the predominant fracture orientation interpreted in the FMI logs was N°90°E. In this interval, only a partial agreement with

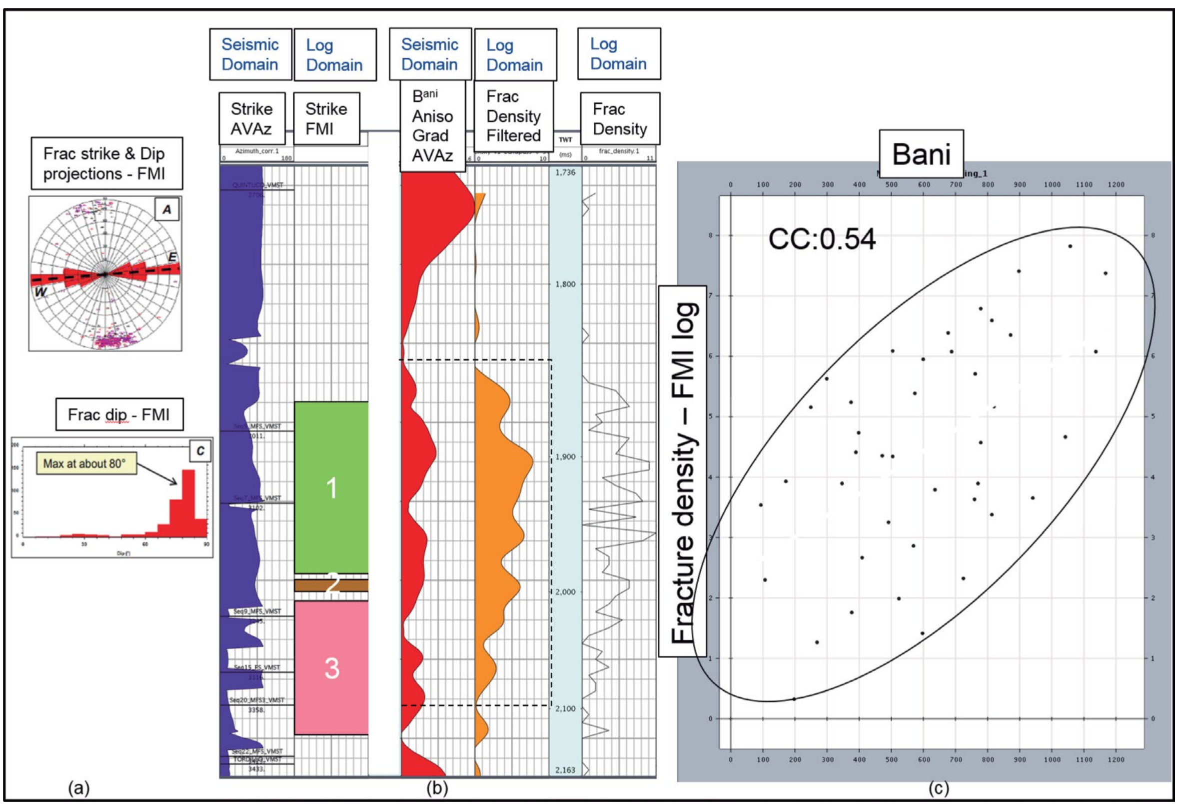

Figure 11. Formation Image Log interpretation at Well-C. Statistical distributions of fracture strike and fracture orientation (a), detailed interpretation as function of depth and comparison with anisotropic attributes derived from azimuthal seismic (b). Crossplot of fracture density (filtered within Far substack seismic bandwidth, high cut: 30 Hz) against Anisotropic gradient from azimuthal seismic in the range of depths displayed in the tracks (c).

the seismic strike is observed, mostly confined from Sequence 9 to Sequence 15.

The anisotropic gradient seems most robust than the orientation. Qualitative agreement is observed in Figure 11b when comparing the Bani trace with the fracture density interpreted from the FMI log filtered in the seismic bandwidth. The crossplot (Figure 11c) shows a clear trend with the higher values of observed fracture density increasing with the anisotropic gradient, Bani. The correlation coefficient obtained (0.54) can be considered as qualitatively good, especially taking into account that the anisotropic gradient is a purely data-driven attribute and no input from well log data is used for its calculation.

In order to map the seismic strike obtained from AVAz into meaningful fracture orientations, a-priori geological constraints must be taken into account to overcome the uncertainty in the computations from equation 1 that allows two possible solutions, φ_0 and φ_0+90°. To guide the solutions we used the minimum curvature attribute to map the fault network. We assume the fracture families will be predominantly oriented with the faults. Then, only solutions of the seismic strike that were consistent with these structural orientations were kept. In practice this implied to sectorize the different maps and to include numerical constraints within the AVAz inversion to map only the geologically consistent strikes per sector. As an example, the minimum curvature at

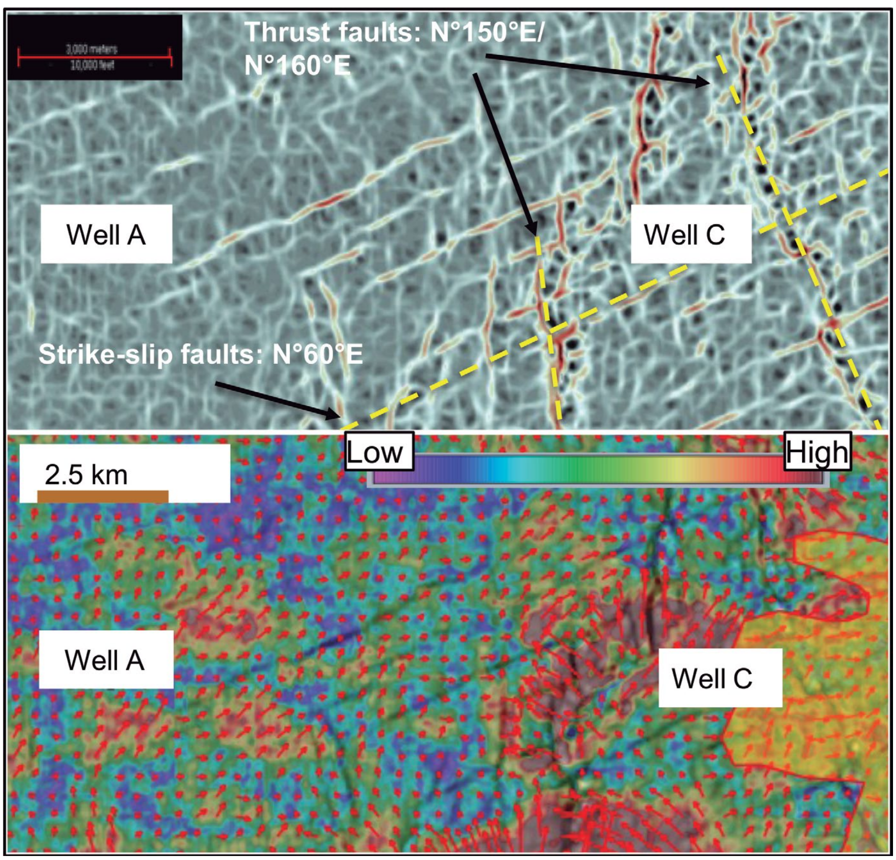

Figure 12. The minimum curvature attribute extracted at Top Tordillo allows characterizing the main faults (top). Anisotropy orientations overlaid with anisotropic gradient and maximum curvature at Top Tordillo (bottom).

Tordillo level is shown in Figure 12, three families of faults are mapped: N°60°E strike-slip faults, N°150°E/N°160°E thrust faults and N°90°E faults, the latter ones are mainly located towards the south of the block (not shown in the figure). The strike-slip and thrust faults are mainly located towards the North-East of the block.

The results for the seismic strike extracted at Tordillo level are shown in Figure 12. They are displayed as arrows scaled by the value of the anisotropic gradient, overlaid with the minimum curvature and the anisotropic gradient.

The results towards the South are biased by the basalts that complicate the interpretation. Only qualitative agreement between the seismic strike and the main faults direction is observed in the data in some areas. The seismic strike should be used with great care and it is not possible to take it as predictive in terms of fracture orientation. It could be useful when combined with a-priori knowledge but even so is noisy and not predictive, at least in this case study.

In terms of lateral variations at target levels, the analysis of the AI and BI was considered more

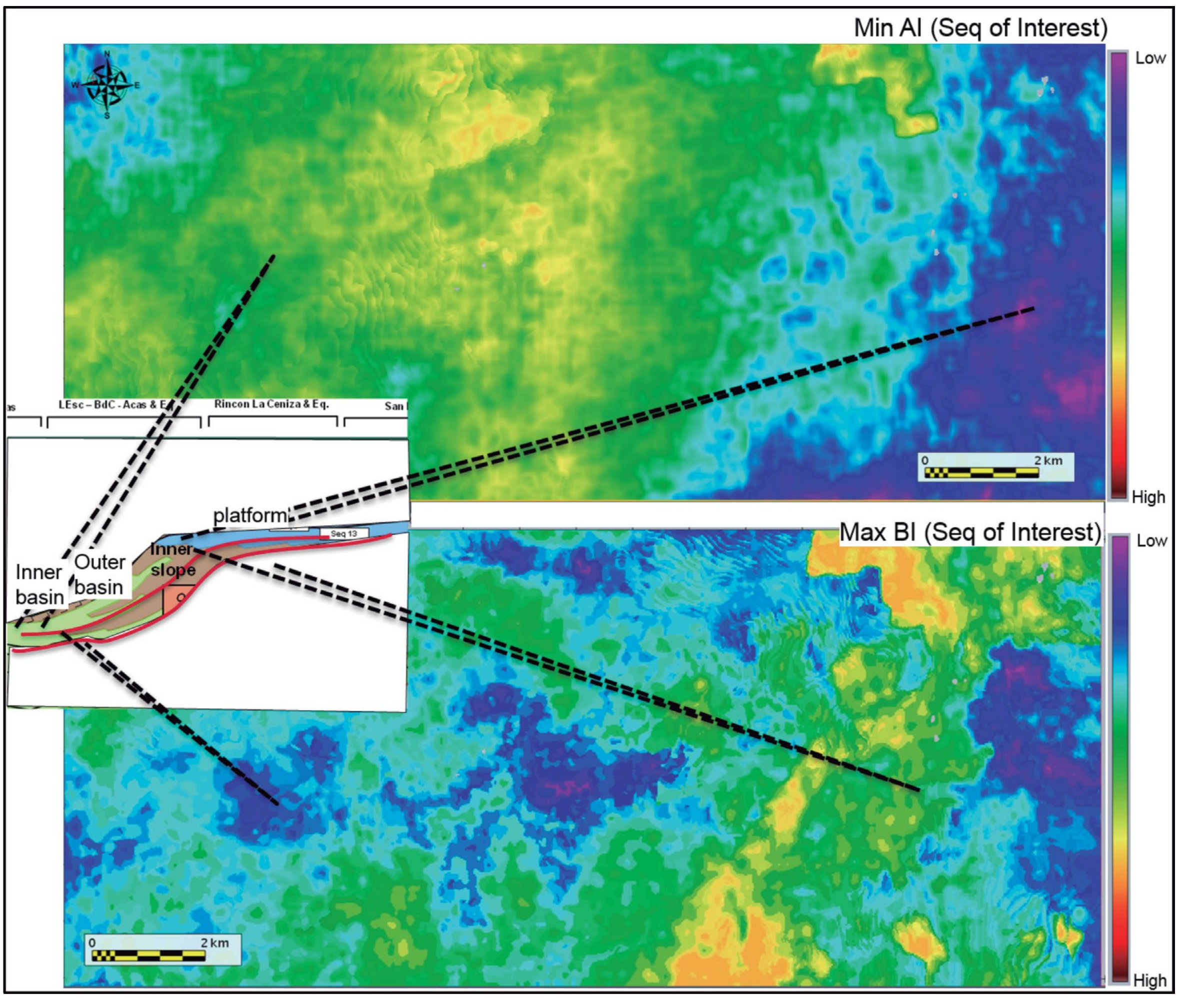

Figure 13. Maps of minimum acoustic impedance (top) and maximum brittleness index (bottom) derived from seismic for the base of a sequence of interest. The AI allows mapping areas of good lithological facies, the BI allows, in principle, mapping areas favorable for hydraulic fracking.

robust. Figure 13 shows the minimum of Acoustic Impedance and the maximum of Brittleness Index in a layer that characterize the base of a Sequence of interest. The AI map shows the degradation of facies towards the West. The brittleness index predicts anomalies in the favorable TOC region that can aid to identify sweet spots to optimize the drilling sequence.

CONCLUSIONS

Thanks to a dedicated WAZ acquisition and a careful processing, the 3D dataset from La Escalonada allows a comprehensive study of elastic and anisotropic attributes in order to assess the potential of seismic data for quantitative reservoir characterization and sweet spots determination.

The acoustic impedance is the main lithological driver, properly discriminating intervals of high TOC and porosity. It is also able to map the carbonate faces which are clearly characterized by high AI values.

The Brittleness Index attribute computed from the elastic inversion showed interesting results in terms of the characterization of brittle intervals and areas. It was able to characterize properly the Quintuco and Tordillo sequences as more brittle and it proved to work better in shaly facies than the anisotropic gradient. It also has a higher resolution than the anisotropic gradient and in layers computations it predicted areas of high brittleness that could be used in combination with the acoustic impedance to identify sweet spots.

From the anisotropic attributes, we concluded that the anisotropic gradient shows an increasing trend West to East which is coherent with formation log image data that showed higher occurrence of fractures in the well located in the East. This anisotropic attribute was also able to characterize known fractured intervals as Tordillo and Quintuco. More importantly, there is a qualitative agreement and a decent correlation with fracture density extracted from the FMI logs. It is important to point out that no log data is used in the computation of the anisotropic gradient so this is an important qualitative validation. The anisotropic gradient seems to characterize fractures better in the carbonate facies than in the shaly facies. The vertical resolution is relatively low and some anomalies cover more than one sequence. This is a consequence of using the Far substack for the AVAz inversion, but this is a price to pay due to the higher sensitivity of the Far substack to fracture density. The analysis of the strike obtained from the AVAz inversion showed that the attribute is noisy and difficult to interpret and conciliate with existing evidence of fractures. Only qualitative agreement in some sequences were found when compared to the fractures orientations from the FMI log and the minimum curvature which shows the main structural directions of the faults and lineaments in the field.

Despite the qualitative agreements, overall the main outcome of the analysis of the anisotropic attributes for fracture characterization was somehow disappointing in this case study.

On the other hand, the attributes derived from the elastic inversion (AI and BI) are more robust than the anisotropic attributes. The joint use of AI and BI has the potential of mapping sweet spots characterized by good petrophysical and lithologic properties with favorable geomechanical conditions for hydraulic fracking.

It is important to keep in mind that a homogeneous fold for the Far substack resulting from a WAZ acquisition is important to obtain high-quality elastic attributes that were later used for the estimation of the brittleness index. In this sense, the extra efforts to acquire WAZ seismic could be worth considering in order to maximize the information from seismic in unconventional reservoirs.

ACKNOWLEDGEMENTS

We are grateful to Total Austral S.A., Shell C.A.P.S.A., O&G and GyP S.A. (Gas y Petróleo del Neuquén S.A.) for facilitating the presentation of this paper. We also thank José Luis Fachal for their valuable improving suggestions and Martin de Santa Coloma and Diego Delucchi for their reading and comments.

REFERENCES

Borgnia, M., 2016, "La Escalonada 3D – Interpretation & P wave acoustic inversion targeting Vaca Muerta", Internal Report – Total Austral.

Cardama, C., C. Strobbia, M. Grausem, P. Ferguson, D. Rojas-Arce, 2015, "3D Seismic Acquisition Focused on Imaging Unconventional Reservoirs", First EAGE/IAPG Workshop on Geophysics for Unconventionals, Buenos Aires, Argentina.

Perez, R. and K. Marfurt, 2014, "Mineralogy-based brittleness prediction from surface seismic data: Application to the Barnett Shale", Interpretation, 2(4), T255-T271.

Pose, F., A. Gangui, and S. Galeazzi, 2014, "Estratigrafía secuencial del intervalo Quintuco-Vaca Muerta en el engolfamiento neuquino, cuenca neuquina, Argentina", IX Congreso de Exploración y Desarrollo de Hidrocarburos, Simposio de Recursos No Convencionales, IAPG, CD Trabajos Tecnicos, Mendoza, Argentina.

Ruger, A., 1997, "P-wave reflection coefficients for transversely isotropic models with vertical and horizontal axis of symmetry", Geophysics, 62, 713–722.

Scott, D.W., 1992, "Multivariate density estimation", John Wiley & Sons, 317 p.

Shuey, R.T., 1986, "A simplification of the Zoeppritz equations", Geophysics, 50, 609-614.

Vargas, R., R. Lotti, A. Pachos, T. Holden, I. Marini, E. Spadafora, J. Pendrel, 2012, "Seismic inversión in the Barnett Shale succesfully pinpoints sweet spots to optimize well-bore placements and reduce drilling risks", SEG Annual Meeting, SEG-2012-1266, Las Vegas, USA.

Wang, F. P., and J. F. W. Gale, 2009, "Screening criteria for shale-gas systems", GCAGS Transactions, 59, 779–793.

10° CONGRESO DE
EXPLORACIÓN Y
DESARROLLO DE
HIDROCARBUROS

Energía y Sociedad
aliados inseparables
Mendoza 2018